Vortex Shedding Intermittency and Its Effects on the Aerodynamics Forces of a Finite-Length Square Cylinder

H.F. Wang, C. Zou and Y.P. Zhang

Abstract The aerodynamic forces on a wall-mounted finite-length square cylinder are experimentally investigated. The width of the tested model $d = 200$ mm, and the aspect ratio $H/d = 5$. The oncoming flow velocity $U_\infty = 13$ m/s, corresponding to a Reynolds number of 1.73×10^5 based on U_∞ and d. It is found that the time-averaged drag coefficient $\overline{C_D}$ and rms value of lift coefficient $C_L^{'}$ of the finite-length cylinder are both smaller than those of 2D square cylinder. Two typical flow modes occur in the flow around the finite-length cylinder: Mode 1 is characterized by alternating spanwise vortex shedding, corresponding to a higher drag and large amplitude fluctuation of lift; Mode 2 is characterized by symmetrical vortex shedding, corresponding to a lower drag and the lift without periodic fluctuation. At the lower part of cylinder, $C_L^{'}$ of Mode 1 is about one times larger than that of Mode 2, this difference reduces gradually with approaching to the free end. The spanwise correlation of aerodynamic force is stronger in Mode 1.

1 Introduction

Finite-length cylinders with one end mounted on a flat wall and the other free are frequently encountered in engineering applications, such as chimneys, cooling towers and high-rise buildings. Under the effects of boundary layer on the wall and cylinder free end, the flow around a finite-length cylinder is highly three dimensional and drastically different from that of a 2D cylinder (Wang and Zhou 2009). In the finite-length cylinder wake, there is a pair of streamwise vortices near the free end, i.e. tip vortices, which induces strong downwash flow. There will be a pair of

Financial support from the NSFC 11472312, 51108468 is acknowledged.

H.F. Wang (✉) · C. Zou · Y.P. Zhang
School of Civil Engineering, Central South University, Changsha, Hunan, China
e-mail: wanghf@csu.edu.cn

Y. Zhou et al. (eds.), *Fluid-Structure-Sound Interactions and Control*,
Lecture Notes in Mechanical Engineering,
DOI 10.1007/978-3-662-48868-3_66

base vortices, if the thickness on the boundary layer is large enough, which results in an upwash flow in the cylinder near wake (Summer et al. 2004; Wang et al. 2006). Under the effects of both tip vortices and base vortices, the spanwise vortices in the finite-length cylinder wake are weakened relative to those in 2D cylinder wake. Furthermore, the width of the near wake of finite-length cylinder is larger and its vortex shedding frequency is lower relative to that of 2D cylinder (Wang and Zhou 2009).

Both the time-averaged drag coefficient $\overline{C_D}$ and fluctuation lift coefficient $C_L^{'}$ of finite-length cylinder are significantly smaller than those of 2D cylinder (Fox and West 1993). Moreover, the $\overline{C_D}$ reduces gradually with decreasing cylinder aspect ratio, H/d, where H is the cylinder height and d is its characteristic width (Okamoto and Sunabashiri 1992). Since the flow around a finite-length cylinder is high three dimensional, the aerodynamics on it are different at various spanwise positions.

Two typical instantaneous flow modes can be identified in the near wake of a finite-length cylinder based on its near wake experimental results for a finite-length square cylinder with $H/d = 4$ and 7 (Wang and Zhou 2009; Bourgeois et al. 2011). Mode 1 is characterized by alternating larger scale spanwise vortices, similar to that in 2D cylinder wake; on the other hand, Mode 2 is dominated by symmetrical spanwise vortices. The two typical modes occur randomly, which must have significant effects on the aerodyanmics forces on the finite-length cylinder.

2 Experimental Details

Experiments were conducted in a closed-loop wind tunnel in Central South University, with a low speed test section of 12 m (width) × 3.5 m (height) × 18 m (length) and a high speed test section of 3 m (width) × 3 m (height) × 15 m (length), respectively. The present experiments were performed in the high speed section.

A finite-length square cylinder with $d = 200$ mm and $H/d = 5$ was mounted on the wind tunnel bottom wall, as shown in Fig. 1a. The oncoming velocity $U_\infty = 13$ m/s, corresponding to $Re = 1.73 \times 10^5$. Pressure taps were arranged at four spanwise positions, i.e. $z^* = 1$, 2.5, 4 and 4.5. The superscript '*' in the present paper indicates normalization with U_∞ and d. All pressure taps were connected to a pressure scanner. For each tap, 20,000 instantaneous samples were measuremed at a frequency of 625 Hz. Measurements were also conducted for a 2D square cylinder at the same Re for comparison. The boundary layer was documented with a Cobra probe prior to the installation of cylinder. As shown in Fig. 1b, the thickness of boundary layer on the wind tunnel wall is about 200 mm, that is most of the tested cylinder is in uniform oncoming flow, except $z^* < 1$.

The time-averaged pressure coefficient $\overline{C_p} = (\overline{P} - P_\infty)/0.5\rho U_\infty^2$, and the rms value of pressure coefficient $C_{p\_rms} = p_{rms}/0.5\rho U_\infty^2$, respectively. In which, $\overline{P}$ is the time-averaged pressure, p_{rms} is the rms value of fluctuation pressure, p_∞ is the static pressure in the wind tunnel.

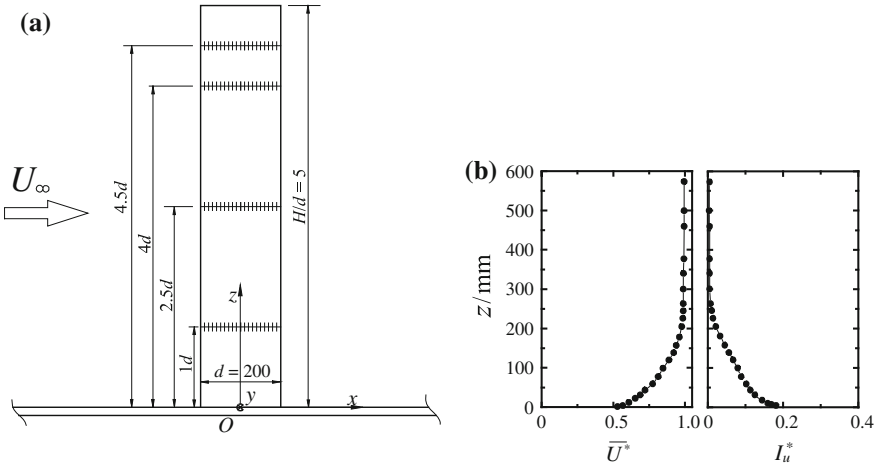

Fig. 1 Experimental setup (**a**) and boundary layer condition (**b**)

3 Results and Discussion

3.1 Time Averaged Results

Figure 2 presents the distribution of $\overline{C_p}$ and C_{p_rms} for both finite length and 2D square cylinder. It can be inferred from Fig. 2 that the $\overline{C_D}$ and $C_L^{'}$ of finite-length cylinder is smaller than those of 2D cylinder. At the windward face (A), $\overline{C_p}$ is quite similar at all spanwise positions, and in line with that of 2D cylinder. On the other hand, the $\overline{C_p}$ on the side faces (B and D) and the leeward face (C) is higher than those of 2D cyinder and quite different at various z^*, i.e., its absolute magnitude is relatively larger near cylinder free end.

For a 2D cylinder, the C_{p_rms} presents the its minimal value at the front stagnation point, and increases quickly with approaching to the side edges. The C_{p_rms} on faces B, D and C is siginificantly larger than that of the cylinder with $H/d = 5$, which may be ascribed to the fact that the spanwise vortex shedding is suppressed in finite-length cylinder wake. The C_{p_rms} at the lower part of the cylinder is relatively larger than that near the cylinder free end, suggesting the suppression of spanwise vortex is more remarkable near cylinder free end under the effects of tip vortices.

3.2 Instantaneous Results

Figure 3 presents the instantaneous C_D and C_L of the finite-length square cylinder and 2D one. The instantaneous pressure coefficients at the centers of both side faces

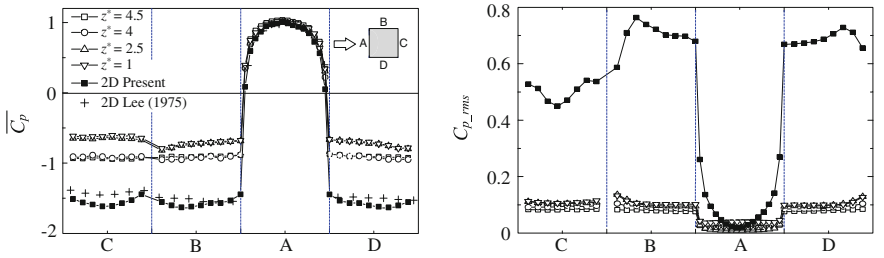

Fig. 2 Distribution of $\overline{C_p}$ and C_{p_rms}

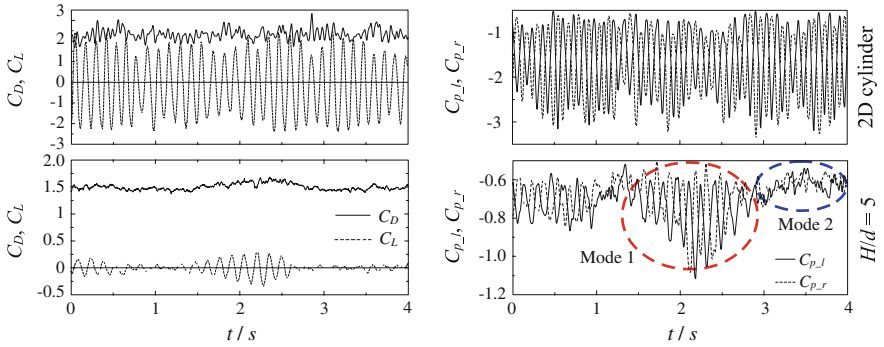

Fig. 3 Instantaneous C_D, C_L and C_p at the center of both side faces

at cylinder midspan, i.e., C_{p_l} and C_{p_r}, are also shown. For the 2D cylinder, C_L presents continues periodic fluctuation, and C_D also fluctuates with a frequency of twice of that of C_L. For the cylinder with $H/d = 5$, the fluctuation of C_L is not continues. This observation should be ascribed to the intermittency of antisymmetrical spanwise vortex shedding, in line with the randomly occurred two typical modes in finite-length cylinder wake (Wang and Zhou 2009; Bourgeois et al. 2011). When antisymmetrical spanwise vortices (Mode 1) occurs, C_L presents periodic fluctuation and the corresponding C_D is relatively larger (1.5–2.5 s); on the other hand, when symmetrical vortices (Mode 2) occurs, C_L has no clear periodicity (2.7–3.5 s). For the 2D cylinder, C_{p_l} and C_{p_r} always are opposite in phase and bear large amplitude fluctuation. For the cylinder with $H/d = 5$, C_{p_l} and C_{p_r} are opposite in phase and fluctuate periodicly when Mode 1 occurs, similar to that for 2D cylinder. On the other hand, C_{p_l} and C_{p_r} do not fluctuate periodicly and have no clear phase relation when Mode 2 occurs, as shown in Fig. 3.

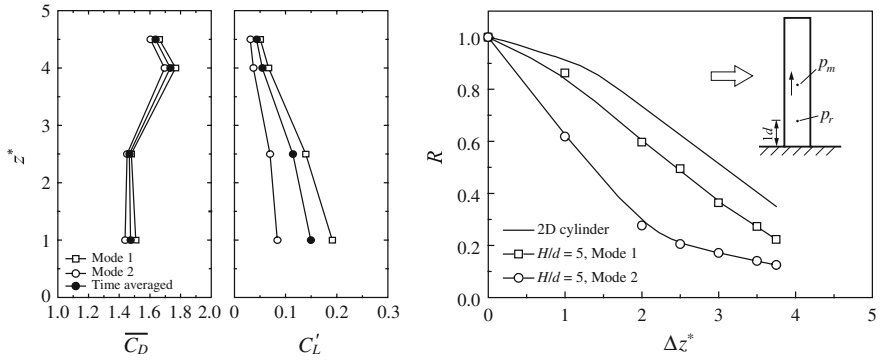

Fig. 4 Conditional averaged $\overline{C_D}$, C_L' and spanwise correlation

3.3 Conditional Averaged Results

In following analysis, we defined the C_L with fluctuation amplitude larger than $1.1\,C_L'$ as Mode 1, otherwise as Mode 2. This criteria was visually chosen so that most large amplitude fluctuation in C_L can be identified as Mode 1. Figure 4 gives the conditional averaged $\overline{C_D}$ and C_L' and also spanwise correlation coefficient R of fluctuation pressure. As shown in Fig. 4, $\overline{C_D}$ of the two typical modes are quite similar, though $\overline{C_D}$ of Mode 1 is slightly larger than that of Mode 2. On the other hand, the difference of C_L' between the two modes is much more significant, especially at the lower part of cylinder. At $z^* = 1$, 2.5, 4 and 4.5, C_L' of Mode 1 is 138, 98, 81 and 65 % larger than that of Mode 2. Under the effects of tip vortices, the difference of C_L' between the two modes reduces gradually with free end approached.

It is also interesting to examine the spanwise correlation of the aerodynamic forces. The reference point is fixed at $z^* = 1$, as shown in Fig. 4. The correlation coefficient R can be determined between the reference point and a moveable point along cylinder span. The spanwise correlation of Mode 1 is also much stronger than that of Mode 2, although both are obviously weaker than that of 2D cylinder.

4 Conclusions

For a finite-length square cylinder in smooth uniform flow, its aerodynamic forces are much smaller than those of 2D cylinder. Two typical modes exist in its near wake. When spanwise vortices are antisymmetrical, i.e. Mode 1, C_L presents large amplitude periodic fluctuation; when symmetrical vortices occur, i.e. Mode 2, C_L has no obvious periodicity and its fluctuation amplitude is limited. The spanwise

correlation of aerodynamic forces in Mode 1 is also significantly stronger than that in Mode 2. Under the effects of tip vortices near cylinder free end, the difference of aerodynamic forces between the two typical modes become less obvious with free end approached.

References

Bourgeois JA, Sattari P, Martinuzzi RJ (2011) Alternating half-loop shedding in the turbulent wake of a finite surface-mounted square cylinder with a thin boundary layer. Phy Fluid 23:095101

Fox TA, West GS (1993) Fluid induced loading of cantilevered circular cylinders in low turbulent uniform flow. Part 2: fluctuating loads with aspect ratios 4 to 25. J Fluid Struct 7:375–386

Okamoto T, Sunabashiri Y (1992) Vortex shedding from a circular cylinder of finite length placed on a ground plane. J Fluid Eng 114:512–521

Summer D, Heseltine JL, Dansereau OJP (2004) Wake structure of a finite circular cylinder of small aspect ratio. Exp Fluids 37:720–730

Wang HF, Zhou Y (2009) The finite-length square cylinder near wake. J Fluid Mech 638:453–490

Wang HF, Zhou Y, Chan CK, Lam KS (2006) Effect of initial conditions on interaction between a boundary layer and a wall-mounted finite-length-cylinder wake. Phy Fluids 18:065106